Chemosphere 291 (2022) 133041

Contents lists available at ScienceDirect

Chemosphere

journal homepage: www.elsevier.com/locate/chemosphere

Electrokinetic remediation for removal of per- and polyfluoroalkyl substances (PFASs) from contaminated soil

Georgios Niarchos [a,*], Mattias Sörengård [b], Fritjof Fagerlund [a], Lutz Ahrens [b]

[a] Uppsala University, Department of Earth Sciences, Uppsala University, P.O. Box 256, SE-751 05, Uppsala, Sweden
[b] Swedish University of Agricultural Sciences, Department of Aquatic Sciences and Assessment, Swedish University of Agricultural Sciences (SLU), P.O. Box 7050, SE-750 07, Uppsala, Sweden

HIGHLIGHTS

- Two novel electrokinetic remediation setups were tested for PFAS-contaminated soil.
- The two-compartment setup resulted in 89% of ∑PFASs accumulation to the anode.
- The single compartment setup resulted in 75% of ∑PFASs removal on GAC.
- Perfluorocarbon chain length affects treatment efficiency for both tested setups.

GRAPHICAL ABSTRACT

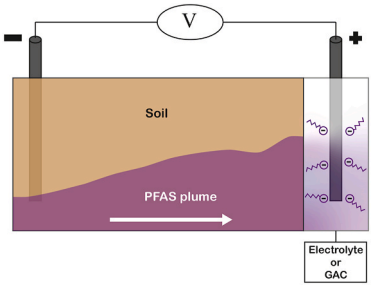

ARTICLE INFO

Handling Editor: X. Cao

Keywords:
Electrokinetics
Treatment
PFAS
Adsorption
Soil
Groundwater

ABSTRACT

Uncontrolled use and disposal of per- and polyfluoroalkyl substances (PFASs) in recent decades has resulted in extensive soil and groundwater contamination, necessitating counteraction. Electrokinetic remediation (EKR) offers a promising approach to *in-situ* soil remediation. Two novel modifications to conventional EKR were tested for the first time in a laboratory-scale study, to explore the capacity of EKR for PFAS removal. The first modification was a two-compartment setup designed for PFAS extraction from soil to an electrolyte-filled chamber. The second was a single-compartment setup designed to transport and confine contaminants in a chamber filled with granular activated carbon (GAC), thus, combining extraction with stabilisation. Electromigration varied for individual compounds, based mainly on perfluorocarbon chain length and functional group. The results indicated up to 89% concentration and extraction of ∑PFASs for the two-compartment setup, with removal efficiency reaching 99% for individual PFASs with $C \leq 6$. Removed PFASs were concentrated adjacent to the anode at the anion exchange membrane, while short-chain compounds were extracted in the anolyte. The single-compartment setup achieved 75% extraction and accumulation of ∑PFASs in GAC. This demonstrates, for the first time, good effectiveness of coupling EKR with AC stabilisation for PFAS removal from soil. Perfluorocarbon chain length was a dominant factor affecting treatment efficiency in both setups, with very high removal rates for short-chain PFASs.

* Corresponding author. Uppsala University, Department of Earth Sciences, P.O. Box 256, SE-751 05, Uppsala, Sweden.
E-mail addresses: georgios.niarchos@geo.uu.se (G. Niarchos), mattias.sorengard@slu.se (M. Sörengård), fritjof.fagerlund@geo.uu.se (F. Fagerlund), lutz.ahrens@slu.se (L. Ahrens).

https://doi.org/10.1016/j.chemosphere.2021.133041
Received 15 September 2021; Received in revised form 16 November 2021; Accepted 20 November 2021
Available online 23 November 2021

1. Introduction

Per- and polyfluoroalkyl substances (PFASs) possess unique non-stick and waterproof properties that have long been utilised in a variety of consumer products and industrial applications, such as aqueous film-forming foams (AFFF) for firefighting (Baduel et al., 2017; Dauchy et al., 2017). Over the past few decades, PFAS disposal was uncontrolled, resulting in ubiquitous environmental contamination (Ahrens, 2011). With mounting evidence of health risks associated with PFASs, especially perfluoroalkyl carboxylic- (PFCAs) and sulfonic acids (PFSAs) (Agency for Toxic Substances and Disease Registry ATSDR, 2021; Pelch et al., 2019; Knutsen et al., 2018), and progressively more regulatory actions being promulgated (Hu et al., 2016; Simon et al., 2019), viable treatment techniques for contaminated environmental media (soil, groundwater) are needed. Remediation of contaminated soils is of paramount importance, since they are major pollution reservoirs from which PFASs can leach into aquifers, eventually compromising drinking water sources (Brusseau et al., 2020).

An increasing variety of treatment approaches for PFAS-contaminated soils are described in the literature. A recent review by Ross et al. (2019) highlighted stabilisation techniques, i.e. containment of contaminants within soil through the use of fixation agents such as activated carbons, as the most mature ones (Ross et al., 2018). Extraction techniques, which instead aim to remove contaminants from the soil, have largely unexplored potential, particularly in the case of PFAS contamination (Sörengård et al., 2019). Electrokinetic remediation (EKR) is a concentration and extraction technique based on the principle that, under the effect of a direct current and low-intensity electric field, charged contaminants will transport towards the electrode of opposite charge (Acar et al., 1995). Transport of the contaminants can consequently result in reduction of the plume size to a confined volume or their eventual extraction from the contaminated media. The technique has several reported advantages over other remediation methods, such as good potential for *in-situ* application, low cost, and good ability to treat low-permeability soils with a high clay content and heterogeneous conditions (Virkutyte et al., 2002; Reddy and Chinthamreddy, 1999; Reddy, 2010). In EKR, mobilisation of contaminants in a porous medium is induced mainly via two mechanisms: electromigration and electroosmosis. Electromigration refers to transportation of contaminants due to an electric field, with cations and anions moving towards the cathode and anode, respectively. Due to their low acid dissociation constant (pK_a) values, PFASs such as PFCAs and PFSAs are typically ionic and specifically anionic under environmental conditions (Ahrens et al., 2012) and can therefore be expected to be transported towards the positively charged anode. Electroosmosis, or electroosmotic flow (EOF), refers to the viscous drag of water particles resulting from the electric field and is typically directed towards the cathode in a negatively charged soil matrix. There can also be minor transport mechanisms at play in EKR, including electrophoresis (i.e. bulk transport of soil particles) and diffusion due to concentration gradients, but these factors can be considered insignificant compared with electroosmosis and electromigration (Baraud et al., 1997). To date, EKR has mainly been applied for removal of inorganic species from soils (Jensen et al., 2007) and studies for the technology's applications for PFASs are limited. In a previous study, we demonstrated that a conventional electrokinetic setup can successfully result in transport of PFASs within a soil column (Sörengård et al., 2019). However, more studies on removal of PFASs using EKR are needed to understand its true potential.

In the present study, we evaluated the effectiveness of two novel EKR setups for removal of PFASs from soil. The first modification was a two-compartment setup designed for extraction of PFASs from soil to an electrolyte-filled chamber. This system allows free movement of hydroxide ions (OH^-) (created at the cathode) into the soil to raise the pH, thus favouring mobilisation of PFASs (Du et al., 2014). Elevated pH can also affect the ionic state of certain PFASs such as perfluorooctane sulfonamide (FOSA), which has a pK_a value of 6.2–6.5 (Rayne and Forest, 2009a), and therefore enhance their potential for electromigration. The second setup tested was a single-compartment setup that coupled electrokinetic transport with sorption of PFASs onto granular activated carbon (GAC), thus inducing a catch and trap effect without the use of an electrolyte. Electrokinetic remediation has been coupled with various permeable reactive barriers in previous studies (Nasiri et al., 2020; Huang et al., 2015, 2019), but to our knowledge this study was the first to investigate coupling electrokinetics with pH control and GAC for PFAS removal from soil.

2. Experimental methods

2.1. Soil sampling and preparation

Two field soils and one artificial soil were used in the experiments. Field soil was sampled at two locations in Sweden (55°43′24.39″N, 13°28′40.88″E (field soil I) and 59°39′43.00477″N, 17°56′11.08658″E (field soil II)). Both sites were adjacent to airports contaminated by PFAS-containing AFFF. After collection, all samples were stored airtight in darkness at 4 °C. Before use, soil lumps were broken down with mortar and pestle, and sieved through a 2 mm sieve and homogenised by end-over-end shaking for 24 h. Artificial soil was used as a control in one experiment. It was prepared in consonance with OECD guidelines (75% quartz sand, 20% kaolinite clay, 5% peat OECD, 1984) and then 10% was spiked with ∑PFASs to a final concentration of 0.06 mg kg^{-1}, i.e. the peat and 5% of the kaolinite clay were spiked with 15 individual PFASs at a starting concentration of 0.6 mg kg^{-1}, to investigate compounds of interest that were not present in the natural field soils (Table 1). The spiked peat and clay were aged for six months prior to the experiments and mixed with the sand and remaining clay for 24 h immediately before the experiments. Before packing the electrokinetic cells with soil, the artificial soil was wet to its water-holding capacity (WHC = 21–35% w/w) to attain saturated conditions. The electrical conductivity of reference soils was used to reflect the ion concentrations (full information on soil characteristics, including electrical conductivity, can be found in Tables S1, S2, S3 and S4 in Supporting Information (SI)).

2.2. Electrokinetic remediation setups

Bench-scale experiments were conducted in cylindrical Plexiglass columns. The soil compartment had a length of 10 cm and a diameter of 8 cm, while the electrolyte and GAC compartment had a length of 5 cm and the same diameter. The distance between the two electrodes, which corresponds to the migration distance, was 13 cm. Direct current (DC) was constantly applied with a power supply (Hewlett Packard E3612A) through carbon rod electrodes (L = 8.5 cm, d = 0.6 cm, surface area = 34.3 cm^2) (SAGITTA, art. No. 84613, Sweden), keeping current constant and having varying voltage. The voltage between the electrodes was monitored throughout the experiments with a multimeter (Uni-T, UT132C Multimeter, Art. No. 48446, China). Electric potential and measured values of other operating parameters are shown in Figs. S1-6 in SI.

2.2.1. Two-compartment EKR

In the two-compartment setup, the goal was to transport PFASs towards the cathode and extract them from soil to the anolyte (Fig. 1). The cathode was inserted in the soil compartment and the anode was inserted in the electrolyte compartment. Hydroxide ions (OH^-) created at the cathode form an alkaline front of higher pH that can move through the soil column towards the positively charged anode, assisting PFAS desorption and removal, since high pH is correlated with higher leachability of PFASs in soils (Campos Pereira et al., 2018). Rehydration of the soil column was achieved by intrusion of the electrolyte through EOF. A chamber filled with electrolyte (sodium nitrate ($NaNO_3$), 0.01 M, VWR, ≥99.5% purity) was attached to the soil chamber, separated from the

soil with a selective anion exchange membrane (AEM) (SUEZ, art. No. AR204SZRA, MKIII, France). The electrolyte was recirculated with a peristaltic pump at a flowrate of 1.8 L h^{-1}. In total, three 21-day experiments were conducted with this setup (experiments A to C), at different current densities and with different soils (two contaminated field soils and an artificial soil spiked with a PFAS mixture) (Table 1). On completion of the experiments, the soil was sliced into 9–10 pieces longitudinally and soil PFAS concentrations were analysed. In experiment C, the concentrations were also measured in the AEM and the anolyte, for the purposes of mass balance analysis. Two different current densities were tested (0.19 and 0.39 mA cm^{-2}), to determine whether higher current density leads to faster ion movement as previously suggested (Hansen et al., 1999). The electric potential varied throughout the experiments, while the current was kept constant.

2.2.2. Single-compartment EKR coupled with GAC

In the single-compartment setup, the anode was inserted directly into the soil, while the cathode was immersed in a chamber of granular activated carbon (GAC) (Filtrasorb 400, 0.55–0.75 mm, bituminous coal). The main aim of this setup (experiment D) was to combine transport of PFASs with their immobilisation on GAC and determine whether GAC can successfully entrap PFASs under the effect of the electric field. The setup was tested using a current density of 0.19 mA cm^{-2}. One of the limitations of EKR is maintenance of saturated conditions for the duration of treatment, since its function depends on the presence of pore fluid (Acar et al., 1995). Therefore, a secondary goal with the single-compartment approach was to estimate the longevity of an electrokinetic setup by letting it operate for as long as possible (91 days) without the use of an electrolyte. After treatment, soil and GAC were sliced into 12 pieces (nine pieces of soil, three pieces of GAC) and the PFAS concentrations in each slice were analysed.

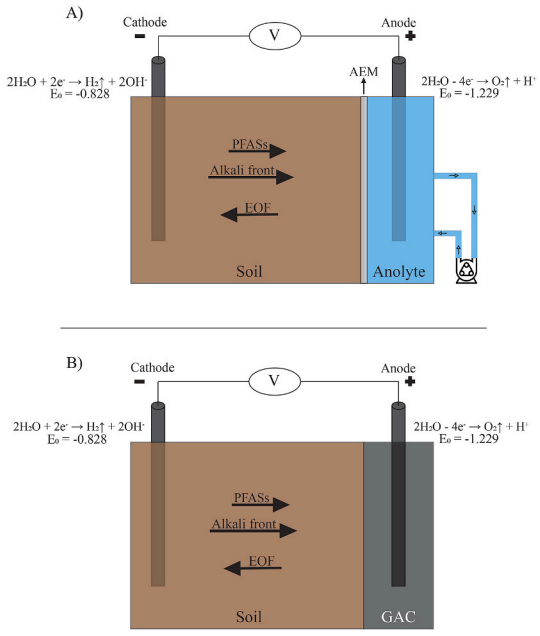

Fig. 1. Schematic representation of A) the two-compartment electrokinetic remediation (EKR) setup (AEM = anion exchange membrane) and B) the single-compartment EKR setup (GAC = granulated activated carbon), showing electrode reactions and transport vectors for per- and polyfluoroalkyl substances (PFASs), electroosmotic flow (EOF) and the alkaline front.

2.3. Analytical standards

The target PFASs were: C_3–C_{11} PFCAs (PFBA, PFPeA, PFHxA, PFHpA, PFOA, PFNA, PFDA, PFUnDA, PFDoDA), C_4, C_6 and C_8 PFSAs (PFBS, PFHxS, PFOS), 6:2, 8:2 and 10:2 fluorotelomer sulfonic acids (FTSAs), C_8 perfluorooctane sulfonamides (FOSA, MeFOSA, EtFOSA), C_8 perfluorooctane sulfonamide ethanols (FOSEs) (MeFOSE, EtFOSE), and C_8 perfluorooctane sulfonamidoacetic acids (FOSAAs) (FOSAA, MeFOSAA, EtFOSAA). The PFASs used for soil spiking (Experiment C) were: PFBA, PFPeA, PFHxA, PFHpA, PFOA, PFNA, PFDA, PFUnDA, PFDoDA, PFBS, PFHxS, PFOS, 8:2 FTSA, 6:2 FTSA, FOSA. In addition, 16 isotopically labelled internal standards (ISs) ($^{13}C_4$-PFBA, $^{13}C_2$-PFHxA, $^{13}C_4$-PFOA, $^{13}C_5$-PFNA, $^{13}C_2$-PFDA, $^{13}C_2$-PFUnDA, $^{13}C_2$-PFDoDA, $^{18}O_2$-PFHxS, $^{13}C_4$-PFOS and $^{13}C_8$-FOSA, D_3-MeFOSA, D_5-EtFOSA, D_7-MeFOSE, D_9-EtFOSE, D_3-MeFOSAA, D_5-EtFOSAA) were used for quantification of PFAS. Further information on recovery rates of the native and internal standards used is provided in Table S5, while all compounds are listed in Tables S6 and S7 in SI.

2.4. PFAS analysis

Soil samples were analysed through soil extraction with methanol and water samples were analysed after centrifugation and filtration as described previously (Ahrens et al., 2009). In brief, freeze-dried soil samples (~2 g) were extracted twice using methanol and the final aliquot was concentrated through N_2 blowdown and filtered through a 0.45 μm recycled cellulose (RC) filter. In experiment B (two-compartment, spiked soil), ion exchange membranes and the electrolyte were also analysed. The extraction procedure for membranes was the same as for soil samples, while the electrolyte samples were injected directly into the analytical instrument after addition of methanol and filtration. PFAS concentrations were quantified using ultra-high performance liquid chromatography coupled to tandem mass spectroscopy (UHPLC-MS/MS) (Quantiva TSQ; Thermo Fisher Scientific, USA), as described elsewhere (Reddy, 2010). For data evaluation, TraceFinder 4.1 was used.

2.5. Soil and water parameters

The characteristics of the soil were determined before and after the experiments, to identify key parameters that could affect the remediation process. Soil texture and carbon content were evaluated as previously described (Sörengård et al., 2019) (Tables S1, S3 in SI). Moisture content was measured gravimetrically in each soil slice after freeze drying. In the two-compartment experiments, electric conductivity of the electrolyte was measured with an EC meter (HI 2211 pH/ORP meter, Hanna Instruments). The results are presented in Figs. S1-6 in SI.

Table 1
Overview of the electrokinetic remediation (EKR) treatments applied in experiments A-D.

Experiment	Current density [mA cm^{-2}]	Duration [d]	Average power consumption[a] [kWh]	Soil origin	Setup
A	0.19	21	0.30	Field soil I	Two-compartment
B	0.39	21	0.55	Field soil II	Two-compartment
C	0.19	21	0.14	Artificial spiked soil[b]	Two-compartment
D	0.19	91	4.73	Field soil II	Single compartment

[a] Average power consumption was calculated using average voltage throughout the experiments.
[b] Artificial soil spiked with PFBA, PFPeA, PFHxA, PFHpA, PFOA, PFNA, PFDA, PFUnDA, PFDoDA, PFBS, PFHxS, PFOS, 8:2 FTSA, 6:2 FTSA, FOSA to ∑PFASs = 0.6 mg kg^{-1}.

2.6. Quality control and quality assurance

Glassware, plastic tubes and experimental equipment that came into contact with soil were rinsed with methanol three times before use. An internal standard (IS) method was used to monitor and improve analytical precision. Average recovery of ISs was 112% ± 38% for the solid phase samples and 84% ± 22% for the liquid phase samples. Analyte-free method blanks (n = 3) were included in the analysis to investigate blank contamination. Blank concentrations were <1% of concentrations detected in the experiments, and thus no blank correction was performed. The method detection limit (MDL) for each target PFAS compound was calculated as $MDL = mean_{blanks} + 3^{*}\sigma_{blanks}$ when concentrations were found in the method blanks, or using the lowest point of a 9-point calibration curve (0.01–100 ng mL^{-1}) in the absence of method blank concentrations (Table S8 in SI). All samples were analysed in triplicate and the standard deviation of replicates was taken to represent the analytical error. Statistical analysis was conducted with ANOVA, applying significance level $\alpha = 0.05$.

3. Results and discussion

3.1. Operating conditions

The two-compartment setup successfully resulted in elevated pH, especially near the cathode, leading to creation of an alkaline front. Specifically, the soil pH ranged from 3.3 at the anode to 10 at the cathode, following a similar trend in all two-compartment experiments (A-C) (Fig. S4 in SI). Similar pH control has been reported for a two-compartment EKR setup when using cation exchange membranes for acidification of sediments (Pedersen et al., 2015). During the experiments, loss of the electrolyte solution was monitored in experiments A and C. Maximum cumulative loss of electrolyte solution was found to be 100 mL after 21 days (~4.8 mL d^{-1}) (Fig. S5 in SI). This volume loss may have been caused by electrolytic reactions taking place at the anode, i.e. water splitting (Fig. 1), or by EOF. On comparing the water profile before and after treatment an effect of EOF was detected, with higher water content at the cathode in all experiments (Fig. S1 in SI). Notably, a 10% increase in soil water content was observed in experiment C by the end of the treatment period, indicating intrusion of the electrolyte into the soil column due to EOF (Fig. S1 in SI). This correlated with the loss of electrolyte solution recorded during the experiments (Fig. S5 in SI). The artificial soil used in experiment C had a higher sand content than the natural soils (I, II) and thus larger pore size, which could have resulted in higher susceptibility to EOF. The electric conductivity of the soil was higher adjacent to the electrodes by the end of the experiments (Fig. S6 in SI), which can be indicative of ion depletion between the electrodes, generation of ions at the electrodes through reactions or increased solubility of ions at the electrodes. Lower electrical conductivity in the pore water between the electrodes can hinder electromigration and increase power consumption. Electric potential fluctuated from 11 to 90 V throughout the two-compartment experiments (A-C), although it was lowest in experiment C, possibly due to higher water content (Fig. S2 in SI). In the single-compartment experiment (D), electric potential reached its maximum (204 V) after 74 days, indicating a resistance increase from depletion of available soil ions (Fig. S3 in SI). This indicates that eventually electrokinetic treatment stops if no recirculation or addition of ions is induced.

3.2. Two-compartment setup

In total, 14 and seven individual PFASs were found to be present in concentrations above MDLs in reference samples of field soils I and II, respectively. Additional PFASs (PFBA, PFNA, PFDA, PFUnDA, 10:2 FTSA) were detected in some soil slices after treatment, notably on the AEM, indicating the presence of PFASs at undetectable levels in the reference soils (Table S2 in SI). Increased concentrations of shorter PFASs could also be due to degradation of precursors or longer-chain PFASs, which has been reported for anodic potential higher than 2.5[30]. However, as Sharma et al. have reviewed (Sharma et al., 2022), degradation and mineralisation of PFASs as a result of electrolysis has only been reported at much higher current densities (≈5–20 mA cm^{-2}), 1–2 orders of magnitude higher than those tested here (0.19–0.39 mA cm^{-2}) and with different types of electrodes and configurations. Concentrations of individual PFASs ranged between 0.15 and 9.4 μg kg^{-1} for field soil I and between 0.07 and 9.7 μg kg^{-1} for field soil II (Table S2 in SI). PFOS displayed the highest concentration in both soils (9.4 and 9.7 μg kg^{-1} for field soil I and II representing 27% and 66% of the sum of the detected PFASs, respectively), exceeding Swedish guidelines for protection of soil for sensitive land use (Pettersson et al., 2015).

A significant increasing trend in PFAS concentration towards the anode due to electromigration was observed in experiments A and B after 21 days of applying direct current ($p < 0.05$, ANOVA for a linear increase). The trend was roughly linear until a depletion started to develop (Fig. 2c, e), followed by an accumulation front with higher rate of mass transport. While an electromigration trend was observed for all PFASs, the extent of transport varied between compounds, with shorter-chain PFASs and PFSAs being more susceptible, both accumulating more in the soil close to the anode and some were small enough to pass through the anion exchange membrane while others were deposited on the membrane (Fig. 3). The lowest reductions in total soil concentrations were found for PFDA, PFUnDA, PFDoDA and FOSA (Fig. 4). Conversely, the removal efficiency, defined as $\frac{C-C_0}{C}$*100% (where C_0 and C are the starting and final PFAS concentrations in the soil within 5 cm of the cathode, respectively), for compounds with $C < 8$ was much higher (in the range 85–99%) than for compounds with $C \geq 8$ (in the range 2.8–30%) (Table S9 in SI). The sorption strength of short-chain PFASs is low (Du et al., 2014), increasing their susceptibility to electromigration. FOSA, which is typically non-ionic at low pH due to its relatively high pK_a of 6.2–6.5 (Rayne and Forest, 2009b), was removed at a low rate (5.3%) from the soil based on its transport gradient, indicating mobilisation due to the electric field (Fig. 2). This can be attributed to alkalinisation of the soil, resulting in ionisation of FOSA (Sörengård et al., 2019). Therefore, higher pH could have possibly resulted in even higher removal rates for FOSA. There were no significant differences in electromigration of PFASs at the higher current density tested in experiment B (Fig. 2). Specifically, 74% of ∑PFASs were concentrated within 5 cm of the anode in experiment B, compared with 68% in experiment A. This difference can be attributed to the different PFAS profiles in the two field soils and the fact that the soil in experiment B had lower organic carbon content, leading to higher potential for desorption. Higher current was therefore not correlated with higher removal rates, contradicting previous results for EKR of heavy metals (Hansen et al., 1999).

To get a complete picture of electromigration patterns, the mass balance of the system was calculated. As was evident in the spiked soil experiment C, (Fig. 4), the soil concentrations of PFASs detected after treatment were lower than the starting concentrations, indicating extraction of PFASs from the soil to the electrolyte or AEM. Mass distribution among different components for experiment B showed almost complete accumulation of PFASs (89%) towards the anode, including soil adjacent to the anode, the AEM and anolyte (Fig. 3). Specifically, 16% of PFASs were detected on the AEM, 13% at the electrolyte, and 61% in soil that was within 5 cm of the anode. The PFASs that were extracted from soil and detected in the electrolyte were mainly PFCAs with $C \leq 6$ and PFHxS. Short and ultra-short chain PFASs are less likely to form aggregates through micelle and hemi-micelle formation (Ateia et al., 2019), and are therefore more likely to pass through the AEM. Some PFASs that were undetectable in the reference soil or negative blanks were observed at the AEM. Notably, among the 17 PFASs detected, five (i.e. PFBA, PFNA, PFDA, PFUnDA, 10:2 FTSA) found at the AEM were previously undetected, indicating either accumulation of these compounds or potential degradation of longer-chain PFASs to

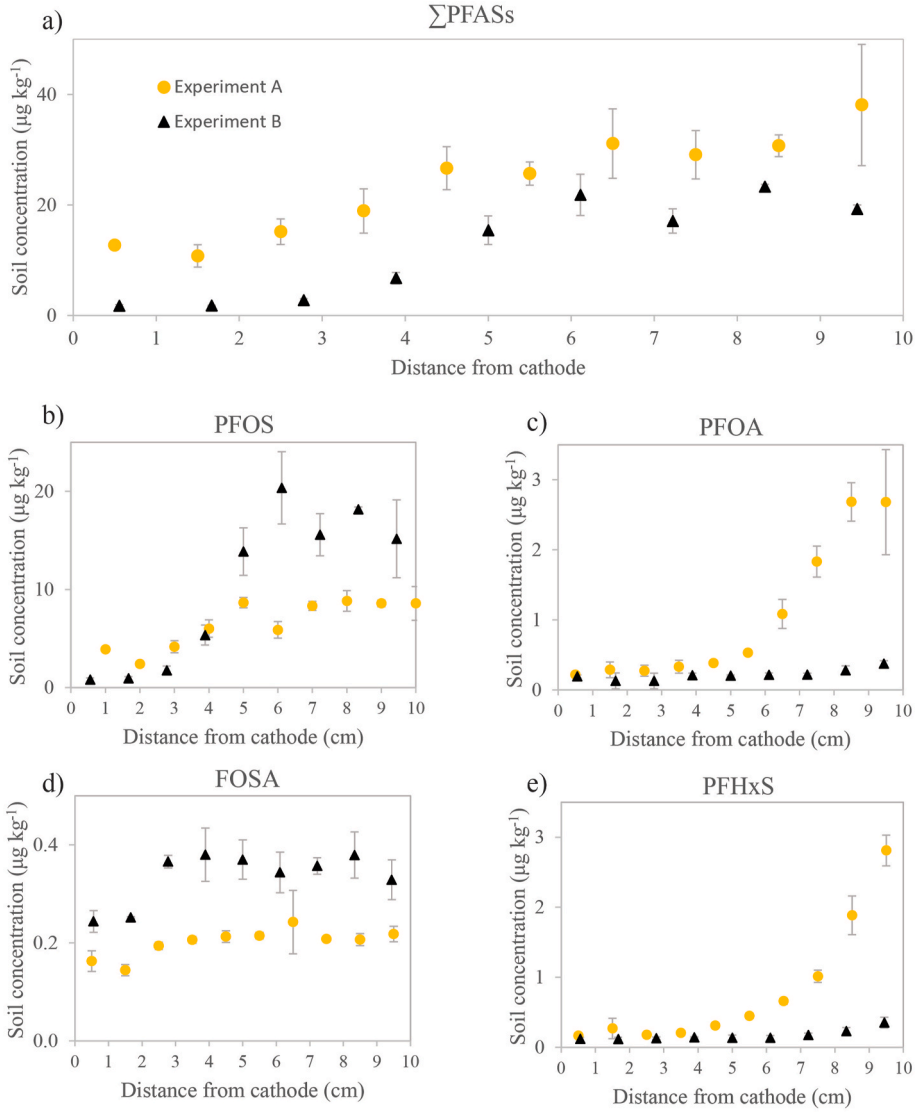

Fig. 2. Transport of a) ∑PFASs, b) PFOS, c) PFOA, d) FOSA and e) PFHxS after 21 days treatment in experiment A (●, field soil I, 0.19 mA cm^{-2}) and experiment B (▲, field soil II, 0.39 mA cm^{-2}) for two field contaminated soils.

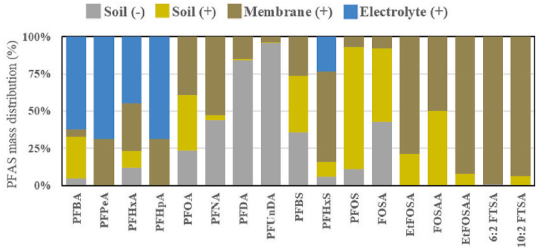

Fig. 3. Mass distribution of individual per- and polyfluoroalkyl substances (PFASs) among different components of the two-compartment setup in experiment B (21 days, 0.39 mA cm^{-2}). Soil (+) and Soil (−) refer to portions of soil within 5 cm of the anode and cathode, respectively.

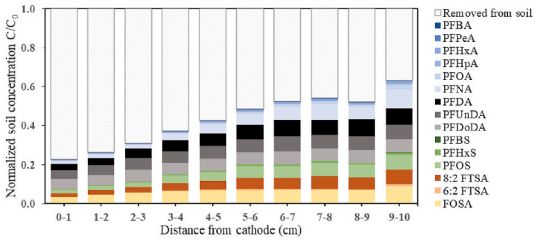

Fig. 4. Longitudinal normalised distribution of individual per- and polyfluoroalkyl substances (PFASs) in experiment C (two-compartment, spiked soil, 0.19 mA cm^{-2}) after 21 days of electrokinetic remediation (EKR). Each PFAS concentration was divided by its background soil concentration in positive controls; $C/C_0 = 1$ corresponds to starting concentration for the sum of 15 PFASs.

shorter-chain compounds. In experiment C, removal efficiency of PFASs was significantly correlated with perfluorocarbon chain length ($p < 0.05$, ANOVA for PFCAs). Removal efficiency exceeded 85% for $C \leq 7$, but then dropped sharply to less than 6% for $C \geq 9$ (Fig. 5). This agrees with other studies showing a sharp increase of PFAS sorption for $C > 7$ (Nguyen et al., 2020; Sörengård et al., 2019, 2020a), indicating an inverse correlation between sorption strength and electromigration. PFASs with different functional groups but similar perfluorocarbon chain length exhibited similar removal efficiencies. Thus, perfluorocarbon chain length appeared to be the dominant factor affecting electromigration. The two-compartment setup did not prove to be efficient for long-chain PFASs such as PFUnDA (4.7%) but was very efficient for

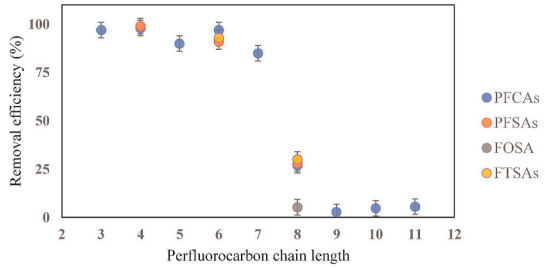

Fig. 5. Removal efficiency as a function of perfluorocarbon chain length in experiment C (two-compartment, spiked artificial soil, 0.19 mA cm^{-2}). Removal is defined as PFASs extracted from soil within 5 cm of the anode, comparing final and starting concentrations.

short-chain PFASs such as PFBS (99%). Short-chain PFASs are much more mobile, due to their higher solubility (Brendel et al., 2018), and therefore transport is much more rapid. Compared with the conventional EKR setup tested in a previous study (Sörengård et al., 2019), the two-compartment setup achieved slightly better overall results, notably for short-chain PFCAs (35–67% higher electrolyte concentrations than previously reported).

3.3. Single-compartment setup

In the single-compartment setup, 75% accumulation for ∑PFASs in the GAC compartment was measured post-treatment (Fig. 6). Only PFOS, FOSA and PFBS were detected in the soil within 5 cm of the cathode, while the other PFASs had been transported towards the anode, indicating almost complete depletion of PFASs at the cathode after treatment. The highest accumulation was observed for PFHpA, which was only detected in the GAC, while PFOS and FOSA accumulated at lower rates (53% and 18%, respectively). They were the largest of the compounds detected (C = 8), which can explain the lower accumulation rate. However, 28% of the remaining PFOS were detected within 5 cm of the anode and only 19% remained within 5 cm of the cathode after treatment. Hence, PFOS transport was evident, but at a lower rate.

The lowest rate of GAC accumulation was seen for FOSA, possibly due to inability of the single-compartment setup to raise the pH and cause ionisation of FOSA. Among the three slices of GAC analysed, PFASs were only detected in the slice that was closest to the soil, indicating strong sorption on GAC and showing that the electric field interferes with the sorption process to a lesser extent in GAC than in soil. However, a trade-off between electromigrative desorption of PFASs from soil and adsorption to GAC is still expected. It is likely that oversaturation of the GAC with PFASs would eventually result in their transport further into the GAC compartment, especially for short- and medium-chain PFCAs (McCleaf et al., 2017).

Overall, the single-compartment setup demonstrated slightly lower removal efficiencies than the two-compartment setup, despite the

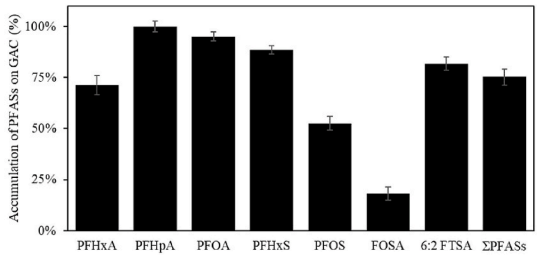

Fig. 6. Accumulation of per- and polyfluoroalkyl substances (PFASs) on granulated activated carbon (GAC) after 91 days of application of 0.19 mA cm^{-2} in a single-compartment setup, based on mass balance. Error bars show average standard deviation of triplicates.

prolonged treatment period. The maximum voltage was reached at 71 days, after which the current density dropped gradually, with EKR of the soil thus ceasing (Fig. S3 in SI). Increase of voltage can result in higher treatment costs, therefore shorter treatment times might be required in a full-scale scenario. The simplicity of the single-compartment setup is an evident advantage, since it can operate without addition and recirculation of electrolyte or the need for ion exchange membranes, which lowers the installation and upkeep costs. In addition, GAC makes for a safer inventory for PFASs compared with electrolyte, since GAC has strong affinity to a wide number of PFASs (Ochoa-Herrera and Sierra-Alvarez, 2008).

3.4. Knowledge gaps and environmental implications

To fully comprehend the capabilities of electrokinetic systems in remediation of PFAS-contaminated soil, further research is required. One important aspect is the kinetics of the electromigration process, knowledge of which could help estimate the method's required treatment times and thus its costs. The electrode spacing could also influence the method's efficiency, as has been recently suggested for petroleum contaminants, where shorter spacing is correlated with higher removal rates (Gidudu and Chirwa, 2020). Although our results did not indicate PFAS degradation based on the mass balance, there could be such an effect at higher current densities, an issue which needs to be investigated in the future. Ultimately, the two-compartment setup resulted in a drastic increase in soil pH close to the cathode (pH = 9–10), which might not be acceptable at every site. Alkalinisation of the soil at the anode could potentially result in precipitation of metals (Król et al., 2020) and a subsequent decrease in conductivity, which would result in an increase in electric potential, and also increasing power consumption. However, the experiments were functional within normal voltage limits and the resistivity even declined during the experiments, possibly due to hydration of the soil. Such parameters would need to be fully understood before full-scale application of the process. In a field-scale application, the effect of groundwater flow should also be considered, as it can potentially disrupt the extent of electromigration. However, the electrodes can also be placed in a way that groundwater flow can be used synergistically (cathode upstream, anode downstream), to cancel the effect of EOF and facilitate the extraction of PFASs. Safety considerations of the electrokinetic method should be further investigated, since the high voltages tested herein could be harmful to living beings. The electric potential reached high levels, however, the current density was still generally low. Therefore, a risk assessment of potential health risks could facilitate the application of the technology at larger scales.

Based on the results, EKR can be a viable treatment option for PFAS-contaminated soils, either when applied alone or in combination with other techniques. The results indicated that EKR can be used to treat a PFAS plume in a contaminated soil either by diverging it or by extracting it from soil to electrolyte or to GAC. EKR can thus help reduce costs related to PFAS destruction, for instance by reducing the contaminant plume that requires thermal destruction (Sörengård et al., 2020b). The two novel setups tested showed high removal rates, especially for short-chain PFASs, while functional groups did not appear to be of major significance. EKR can therefore be a promising solution for removal of short-chain compounds, which can pose a challenge for other soil remediation techniques such as stabilisation and thermal destruction (Du et al., 2014; Gagliano et al., 2020; Watanabe et al., 2016). Removal of long-chain PFASs from contaminated media is a more challenging task, but combining EKR with other techniques (e.g. stabilisation (Ross et al., 2018)) could potentially increase the removal efficiency for these compounds. Therefore, the specific PFAS composition at a particular contaminated site must be considered before applying EKR. In view of the worldwide switch to production and use of short-chain PFASs, extraction techniques such as EKR may become particularly relevant in the future. Further studies should therefore focus on optimisation and upscaling of the EKR process.

Funding sources

This work was financially supported partly by VINNOVA through the PFAS-PURE project (2015–03561) and partly by TUFFO – a research and innovation program on contaminated sites managed by the Swedish Geotechnical Institute (SGI) – through the StopPFAS project.

Author contributions

Author 1: **Georgios Niarchos**. - Conceived and designed the analysis. - Performed the experiments. - Collected the data. - Performed the analysis. - Wrote the paper (Drafted the manuscript and applied revisions). Author 2: **Mattias Sörengård**. - Conceived and designed the analysis. - Contributed data. - Offered a critical revision of the article, including data interpretation. Author 3: **Fritjof Fagerlund**. - Conceived and designed the analysis. - Offered a critical revision of the article, including data interpretation. Author 4: **Lutz Ahrens**. - Conceived and designed the analysis. - Contributed analysis tools. - Offered a critical revision of the article, including data interpretation.

Declaration of competing interest

The authors declare that they have no known competing financial interests or personal relationships that could have appeared to influence the work reported in this paper.

Appendix A. Supplementary data

Supplementary data to this article can be found online at https://doi.org/10.1016/j.chemosphere.2021.133041.

References

Acar, Y.B., Gale, R.J., Alshawabkeh, A.N., Marks, R.E., Puppala, S., Bricka, M., Parker, R., 1995. Electrokinetic remediation: basics and technology status. J. Hazard Mater. 40 (2), 117–137. https://doi.org/10.1016/0304-3894(94)00066-.

Agency for Toxic Substances and Disease Registry (ATSDR), 2021. Toxicological profile for Perfluoroalkyls. Department of Health and Human Services, Public Health Service, Atlanta, GA: U.S. https://doi.org/10.15620/cdc:59198.

Ahrens, L., 2011. Polyfluoroalkyl compounds in the aquatic environment: a review of their occurrence and fate. J. Environ. Monit. 13 (1), 20–31. https://doi.org/10.1039/C0EM00373E.

Ahrens, L., Felizeter, S., Sturm, R., Xie, Z., Ebinghaus, R., 2009. Polyfluorinated compounds in waste water treatment plant effluents and surface waters along the river elbe, Germany. Mar. Pollut. Bull. 58 (9), 1326–1333. https://doi.org/10.1016/j.marpolbul.2009.04.028.

Ahrens, L., Harner, T., Shoeib, M., Lane, D.A., Murphy, J.G., 2012. Improved characterization of gas-particle partitioning for per- and polyfluoroalkyl substances in the atmosphere using annular diffusion denuder samplers. Environ. Sci. Technol. 46 (13), 7199–7206. https://doi.org/10.1021/es300898s.

Ateia, M., Maroli, A., Tharayil, N., Karanfil, T., 2019. The overlooked short- and ultrashort-chain poly- and perfluorinated substances: a review. Chemosphere 220, 866–882. https://doi.org/10.1016/j.chemosphere.2018.12.186.

Baduel, C., Mueller, J.F., Rotander, A., Corfield, J., Gomez-Ramos, M.-J., 2017. Discovery of novel per- and polyfluoroalkyl substances (PFASs) at a fire fighting training ground and preliminary investigation of their fate and mobility. Chemosphere 185, 1030–1038. https://doi.org/10.1016/j.chemosphere.2017.06.096.

Baraud, F., Tellier, S., Astruc, M., 1997. Ion velocity in soil solution during electrokinetic remediation. J. Hazard Mater. 56 (3), 315–332. https://doi.org/10.1016/S0304-3894(97)00073-3.

Brendel, S., Fetter, É., Staude, C., Vierke, L., Biegel-Engler, A., 2018. Short-chain perfluoroalkyl acids: environmental concerns and a regulatory strategy under REACH. Environ. Sci. Eur. 30 (1), 9. https://doi.org/10.1186/s12302-018-0134-4.

Brusseau, M.L., Anderson, R.H., Guo, B., 2020. PFAS concentrations in soils: background levels versus contaminated sites. Sci. Total Environ. 740, 140017. https://doi.org/10.1016/j.scitotenv.2020.140017.

Campos Pereira, H., Ullberg, M., Kleja, D.B., Gustafsson, J.P., Ahrens, L., 2018. Sorption of perfluoroalkyl substances (PFASs) to an organic soil horizon – effect of cation composition and PH. Chemosphere 207, 183–191. https://doi.org/10.1016/j.chemosphere.2018.05.012.

Dauchy, X., Boiteux, V., Bach, C., Rosin, C., Munoz, J.-F., 2017. Per- and polyfluoroalkyl substances in firefighting foam concentrates and water samples collected near sites impacted by the use of these foams. Chemosphere 183, 53–61. https://doi.org/10.1016/j.chemosphere.2017.05.056.

Du, Z., Deng, S., Bei, Y., Huang, Q., Wang, B., Huang, J., Yu, G., 2014. Adsorption behavior and mechanism of perfluorinated compounds on various adsorbents-A review. J. Hazard Mater. 274, 443–454. https://doi.org/10.1016/j.jhazmat.2014.04.038.

Gagliano, E., Sgroi, M., Falciglia, P.P., Vagliasindi, F.G.A., Roccaro, P., 2020. Removal of Poly- and Perfluoroalkyl Substances (PFAS) from Water by Adsorption: Role of PFAS Chain Length, Effect of Organic Matter and Challenges in Adsorbent Regeneration. Water Research. Elsevier Ltd March 15, p. 115381. https://doi.org/10.1016/j.watres.2019.115381.

Gidudu, B., Chirwa, E.M.N., 2020. The combined application of a high voltage, low electrode spacing, and biosurfactants enhances the bio-electrokinetic remediation of petroleum contaminated soil. J. Clean. Prod. 276, 122745. https://doi.org/10.1016/j.jclepro.2020.122745.

Hansen, H.K., Ottosen, L.M., Hansen, L., Kliem, B.K., Villumsen, A., Bech-Nielsen, G., 1999. Electrodialytic remediation of soil polluted with heavy metals. Key parameters for optimization of the process. Chem. Eng. Res. Des. 77 (3), 218–222. https://doi.org/10.1205/026387699526124.

Hu, X.C., Andrews, D.Q., Lindstrom, A.B., Bruton, T.A., Schaider, L.A., Grandjean, P., Lohmann, R., Carignan, C.C., Blum, A., Balan, S.A., Higgins, C.P., Sunderland, E.M., 2016. Detection of poly- and perfluoroalkyl substances (PFASs) in U.S. Drinking water linked to industrial sites, military fire training areas, and wastewater treatment plants. Environ. Sci. Technol. Lett. 3 (10), 344–350. https://doi.org/10.1021/acs.estlett.6b00260.

Huang, T., Li, D., Kexiang, L., Zhang, Y., 2015. Heavy metal removal from MSWI fly ash by electrokinetic remediation coupled with a permeable activated charcoal reactive barrier. Sci. Rep. 5 (1), 1–16. https://doi.org/10.1038/srep15412.

Huang, T., Liu, L., Zhang, S., Xu, J., 2019. Evaluation of electrokinetics coupled with a reactive barrier of activated carbon loaded with a nanoscale zero-valent iron for selenite removal from contaminated soils. J. Hazard Mater. 368, 104–114. https://doi.org/10.1016/j.jhazmat.2019.01.036.

Jensen, P.E., Ahring, B.K., Ottosen, L.M., 2007. Organic acid enhanced electrodialytic extraction of lead from contaminated soil fines in suspension. J. Chem. Technol. Biotechnol. 82 (10), 920–928. https://doi.org/10.1002/jctb.1762.

Knutsen, H.K., Alexander, J., Barregård, L., Bignami, M., Brüschweiler, B., Ceccatelli, S., Cottrill, B., Dinovi, M., Edler, L., Grasl-Kraupp, B., Hogstrand, C., Hoogenboom, L., Ron, Nebbia, C.S., Oswald, I.P., Petersen, A., Rose, M., Roudot, A., Vleminckx, C., Vollmer, G., Wallace, H., Bodin, L., Cravedi, J., Halldorsson, T.I., Haug, L.S., Johansson, N., van Loveren, H., Gergelova, P., Mackay, K., Levorato, S., van Manen, M., Schwerdtle, T., Schwerdtle, T., 2018. Risk to human health related to the presence of perfluorooctane sulfonic acid and perfluorooctanoic acid in food. EFSA J 16 (12). https://doi.org/10.2903/j.efsa.2018.5194.

Król, A., Mizerna, K., Bożym, M., 2020. An assessment of pH-dependent release and mobility of heavy metals from metallurgical slag. J. Hazard Mater. 384, 121502. https://doi.org/10.1016/j.jhazmat.2019.121502.

McCleaf, P., Englund, S., Östlund, A., Lindegren, K., Wiberg, K., Ahrens, L., 2017. Removal efficiency of multiple poly- and perfluoroalkyl substances (PFASs) in drinking water using granular activated carbon (GAC) and anion exchange (AE) column tests. Water Res. 120, 77–87. https://doi.org/10.1016/j.watres.2017.04.057.

Nasiri, A., Jamshidi-Zanjani, A., Khodadadi Darban, A., 2020. Application of enhanced electrokinetic approach to remediate Cr-contaminated soil: effect of chelating agents and permeable reactive barrier. Environ. Pollut. 266, 115197. https://doi.org/10.1016/j.envpol.2020.115197.

Nguyen, T.M.H., Bräunig, J., Thompson, K., Thompson, J., Kabiri, S., Navarro, D.A., Kookana, R.S., Grimison, C., Barnes, C.M., Higgins, C.P., McLaughlin, M.J., Mueller, J.F., 2020. Influences of chemical properties, soil properties, and solution PH on soil–water partitioning coefficients of per- and polyfluoroalkyl substances (PFASs). Environ. Sci. Technol. 54 (24), 15883–15892. https://doi.org/10.1021/ACS.EST.0C05705.

Ochoa-Herrera, V., Sierra-Alvarez, R., 2008. Removal of perfluorinated surfactants by sorption onto granular activated carbon, zeolite and sludge. Chemosphere 72 (10), 1588–1593. https://doi.org/10.1016/j.chemosphere.2008.04.029.

OECD, 1984. Test No. 207: Earthworm, Acute Toxicity Tests. OECD Guidelines for the Testing of Chemicals, Section 2. OECD Publishing, Paris. https://doi.org/10.1787/9789264070042-en.

Pedersen, K.B., Jensen, P.E., Ottosen, L.M., Lejon, T., 2015. An optimised method for electrodialytic removal of heavy metals from harbour sediments. Electrochim. Acta 173, 432–439. https://doi.org/10.1016/j.electacta.2015.05.050.

Pelch, K.E., Reade, A., Wolffe, T.A.M., Kwiatkowski, C.F., 2019. PFAS Health Effects Database: Protocol Syst. Evid. Map 130, 104851.

Pettersson, M., Ländell, M., Ohlsson, Y., Kleja, D.B., Tiberg, C., 2015. Preliminära Riktvärden För Högfluorerade Ämnen (PFAS) I Mark Och Grundvatten. Linköping.

Rayne, S., Forest, K., 2009a. Perfluoroalkyl sulfonic and carboxylic acids: a critical review of physicochemical properties, levels and patterns in waters and wastewaters, and treatment methods. J. Environ. Sci. Heal. Part A 44 (12), 1145–1199. https://doi.org/10.1080/10934520903139811.

Rayne, S., Forest, K., 2009b. A new class of perfluorinated acid contaminants: primary and secondary substituted perfluoroalkyl sulfonamides are acidic at environmentally and toxicologically relevant PH values. J. Environ. Sci. Heal. - Part A Toxic/Hazardous Subst. Environ. Eng. 44 (13), 1388–1399. https://doi.org/10.1080/10934520903217278.

Reddy, K.R., 2010. Technical challenges to in-situ remediation of polluted sites. Geotech. Geol. Eng. 28 (3), 211–221. https://doi.org/10.1007/s10706-008-9235-y.

Reddy, K.R., Chinthamreddy, S., 1999. Electrokinetic remediation of heavy metal-contaminated soils under reducing environments. Waste Manag. 19 (4), 269–282. https://doi.org/10.1016/S0956-053X(99)00085-9.

Ross, I., McDonough, J., Miles, J., Storch, P., Thelakkat Kochunarayanan, P., Kalve, E., Hurst, J., Dasgupta S, S., Burdick, J., 2018. A review of emerging technologies for

remediation of PFASs. Remed. J. 28 (2), 101–126. https://doi.org/10.1002/rem.21553.

Sharma, S., Shetti, N.P., Basu, S., Nadagouda, M.N., Aminabhavi, T.M., 2022. Remediation of per- and polyfluoroalkyls (PFAS) via electrochemical methods. Chem. Eng. J. 430, 132895. https://doi.org/10.1016/J.CEJ.2021.132895.

Simon, J.A., Abrams, S., Bradburne, T., Bryant, D., Burns, M., Cassidy, D., Cherry, J., Chiang, S., Dora), Cox, D., Crimi, M., Denly, E., DiGuiseppi, B., Fenstermacher, J., Fiorenza, S., Guarnaccia, J., Hagelin, N., Hall, L., Hesemann, J., Houtz, E., Koenigsberg, S.S., Lauzon, F., Longsworth, J., Maher, T., McGrath, A., Naidu, R., Newell, C.J., Parker, B.L., Singh, T., Tomiczek, P., Wice, R., 2019. PFAS experts symposium: statements on regulatory policy, chemistry and analytics, toxicology, transport/fate, and remediation for per- and polyfluoroalkyl substances (PFAS) contamination issues. Remed. J. 29 (4), 31–48. https://doi.org/10.1002/rem.21624.

Sörengård, M., Niarchos, G., Jensen, P.E., Ahrens, L., 2019. Electrodialytic per- and polyfluoroalkyl substances (PFASs) removal mechanism for contaminated soil. Chemosphere 232, 224–231. https://doi.org/10.1016/j.chemosphere.2019.05.088.

Sörengård, M., Östblom, E., Köhler, S., Ahrens, L., 2020a. Adsorption behavior of per- and polyfluoralkyl substances (PFASs) to 44 inorganic and organic sorbents and use of dyes as proxies for PFAS sorption. J. Environ. Chem. Eng. 8 (3), 103744. https://doi.org/10.1016/J.JECE.2020.103744.

Sörengård, M., Kleja, D.B., Ahrens, L., 2019. Stabilization of per- and polyfluoroalkyl substances (PFASs) with colloidal activated carbon (PlumeStop®) as a function of soil clay and organic matter content. J. Environ. Manag. 249, 109345. https://doi.org/10.1016/j.jenvman.2019.109345.

Sörengård, M., Lindh, A.S., Ahrens, L., 2020b. Thermal desorption as a high removal remediation technique for soils contaminated with per- and polyfluoroalkyl substances (PFASs). PLoS One 15 (6 June). https://doi.org/10.1371/journal.pone.0234476.

Virkutyte, J., Sillanpää, M., Latostenmaa, P., 2002. Electrokinetic soil remediation - critical overview. Sci. Total Environ. 289 (1–3), 97–121. https://doi.org/10.1016/S0048-9697(01)01027-0.

Watanabe, N., Takemine, S., Yamamoto, K., Haga, Y., Takata, M., 2016. Residual organic fluorinated compounds from thermal treatment of PFOA, PFHxA and PFOS adsorbed onto granular activated carbon (GAC). J. Mater. Cycles Waste Manag. 18 (4), 625–630. https://doi.org/10.1007/S10163-016-0532-X.